

## Magnetic properties of the Haldane-gap material $[\text{Ni}(\text{C}_2\text{H}_8\text{N}_2)_2\text{NO}_2](\text{BF}_4)$

E Čížmár<sup>1,6</sup>, M Ozerov<sup>1</sup>, O Ignatchik<sup>1</sup>, T P Papageorgiou<sup>1</sup>, J Wosnitzer<sup>1</sup>, S A Zvyagin<sup>1</sup>, J Krzystek<sup>2</sup>, Z Zhou<sup>3</sup>, C P Landee<sup>4</sup>, B R Landry<sup>4</sup>, M M Turnbull<sup>4</sup> and J L Wikaira<sup>5</sup>

<sup>1</sup> Dresden High Magnetic Field Laboratory (HLD), Forschungszentrum Dresden-Rossendorf, 01314 Dresden, Germany

<sup>2</sup> National High Magnetic Field Laboratory, Florida State University, Tallahassee, FL 32310, USA

<sup>3</sup> Department of Physics and Astronomy, Wayne State University, Detroit, MI 48201, USA

<sup>4</sup> Department of Physics and Carlson School of Chemistry, Clark University, Worcester, MA 01060, USA

<sup>5</sup> Department of Chemistry, University of Canterbury, Christchurch, New Zealand

E-mail: [e.cizmar@fzd.de](mailto:e.cizmar@fzd.de)

*New Journal of Physics* **10** (2008) 033008 (9pp)

Received 10 January 2008

Published 6 March 2008

Online at <http://www.njp.org/>

doi:10.1088/1367-2630/10/3/033008

**Abstract.** Results of magnetization and high-field electron spin resonance (ESR) studies of the new spin-1 Haldane-chain material  $[\text{Ni}(\text{C}_2\text{H}_8\text{N}_2)_2\text{NO}_2](\text{BF}_4)$  (NENB) are reported. A definite signature of the Haldane state in NENB was obtained. From the analysis of the frequency–field dependence of magnetic excitations in NENB, the spin-Hamiltonian parameters were calculated, yielding  $\Delta/k_B = 17.4$  K,  $g_{\parallel} = 2.14$ ,  $D/k_B = 7.5$  K and  $|E/k_B| = 0.7$  K for the Haldane gap,  $g$  factor and the crystal-field anisotropy constants, respectively. The presence of fractional  $S = 1/2$  chain-end states, revealed by ESR and magnetization measurements, is found to be responsible for spin-glass freezing effects. In addition, extra states in the excitation spectrum of NENB have been observed in the vicinity of the Haldane gap; their origin is discussed.

<sup>6</sup> Author to whom any correspondence should be addressed.

## Contents

<b>1. Introduction</b>	<b>2</b>
<b>2. Experimental details</b>	<b>2</b>
<b>3. Results and discussion</b>	<b>3</b>
<b>4. Conclusions</b>	<b>8</b>
<b>Acknowledgments</b>	<b>8</b>
<b>References</b>	<b>8</b>

## 1. Introduction

Antiferromagnetic (AFM) quantum spin-1 chains have been the subject of intense theoretical and experimental studies, fostered especially by the Haldane conjecture [1]. In accordance with the valence-bond-solid (VBS) model proposed by Affleck *et al* [2], each  $S = 1$  spin can be regarded as a symmetric combination of two  $S = 1/2$  moments forming a spin-singlet ground state. The value of the energy gap  $\Delta = 0.41 J$  (where  $J$  is the spin–spin exchange coupling) has been estimated for an  $S = 1$  isotropic Heisenberg AFM chain using the density-matrix renormalization-group (DMRG) [3] and exact diagonalization [4] techniques. The presence of the Haldane gap was experimentally revealed in a number of materials (see for instance [5]–[8]). Nowadays, investigations of intriguing properties of Haldane materials (particular their high-field magnetic properties) continue to attract a great deal of attention. For instance, experimental studies of the Haldane materials NDMAP [9, 10] and TMNIN [11] suggest the realization of the Tomonaga–Luttinger-liquid high-field phase [12, 13]. At sufficiently low temperature, an applied magnetic field can induce long-range magnetic order, which can be effectively described as the condensation of a dilute gas of magnons [14, 15].

In this paper, we utilize magnetization and electron spin resonance (ESR) techniques to study the new spin-1 Haldane compound  $[\text{Ni}(\text{C}_2\text{H}_8\text{N}_2)_2\text{NO}_2](\text{BF}_4)$  (abbreviated as NENB). The presence of the Haldane state in NENB has been confirmed experimentally. Analysis of the frequency–field dependence of magnetic excitations in NENB allowed us to determine the spin-Hamiltonian parameters, yielding  $g_{\parallel} = 2.14$ ,  $D/k_{\text{B}} = 7.5 \text{ K}$  and  $|E/k_{\text{B}}| = 0.7 \text{ K}$  for the  $g$  factor and the crystal-field anisotropy constants, respectively. The presence of spin-1/2 excitations in nominally pure NENB crystals revealed by our experimental observations suggested the existence of weakly-interacting antiferromagnet droplets originating from broken spin bonds. In addition, extra states in the excitation spectrum in the vicinity of the Haldane gap were observed; their origin is discussed.

## 2. Experimental details

Single crystals of NENB were grown by the reaction of  $[\text{Ni}(\text{C}_2\text{H}_8\text{N}_2)_3](\text{BF}_4)_2$  with  $\text{Ni}(\text{BF}_4)_2 \cdot 6\text{H}_2\text{O}$  and  $\text{NaNO}_2$  in aqueous solution. Careful slow evaporation in a partially covered container yielded ruby-red crystals of up to 3–4 mm in length and 1–2 mm<sup>2</sup> cross-section. Single-crystal x-ray analysis showed an orthorhombic unit cell, space group  $Pnma$  (similar to that of the isostructural compound  $[\text{Ni}(\text{C}_2\text{H}_8\text{N}_2)_2\text{NO}_2](\text{ClO}_4)$ , abbreviated as NENP [16]), with  $a = 15.0373(5) \text{ \AA}$ ,  $b = 10.2276(3) \text{ \AA}$  and  $c = 7.9719(2) \text{ \AA}$ . Each  $\text{Ni}^{2+}$  ion is pseudo-octahedrally

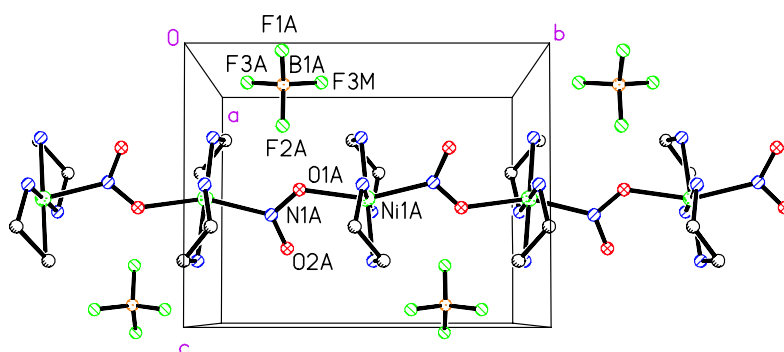


**Figure 1.** The structure of NENB showing the polymeric chain arrangement, the orientation of the nitrite ligands, and the placement of the  $\text{BF}_4$  anions relative to the chain. Atoms are shown as spheres of arbitrary size and hydrogen atoms are not shown for clarity.

coordinated. The four nitrogen atoms of the two ethylenediamine rings (ethylenediamine =  $\text{C}_2\text{N}_2\text{H}_8$ ) make a slightly distorted square planar symmetry with bridging  $\text{NO}_2^-$  ions creating the octahedral axis approximately parallel to the chain direction. The individual chains are well isolated by the inorganic counterions  $\text{BF}_4^-$ . As follows from crystallographical analysis the mean planes of successive  $\text{Ni}^{2+}$  units are canted by an angle of  $14.1^\circ$  to each other. The orientation of the nitrite ions within a single chain appears to be uniform (one N atom and one O atom are coordinated to each  $\text{Ni}^{2+}$  center) as shown in figure 1 (full crystallographic details are available from the Cambridge Crystallographic Data Center, deposition number 637023) [17].

The static susceptibility was measured using a commercial SQUID magnetometer equipped with a 7 T magnet in the temperature range from 1.8 to 300 K. The sample was attached with a small amount of Apiezon N grease to the inside of a straw held by a sample-holder rod. The core diamagnetic contribution to the magnetic moment of the sample, calculated using Pascal's constants [18], was subtracted from the raw data. The magnetization was measured in fields up to 15 T using a torque magnetometer in a dilution refrigerator. ESR experiments were performed in the Voigt geometry with the external field applied along the  $b$ -axis using a tunable-frequency ESR set-up at the National High Magnetic Field Laboratory, Tallahassee [19] and at the Dresden High Magnetic Field Laboratory, Dresden.

### 3. Results and discussion

The zero-field-cooled (ZFC) magnetic susceptibility of NENB measured in a field of  $B = 0.1$  T applied parallel and perpendicular to the  $b$ -axis is shown in figure 2. The pronounced maximum and low-temperature behavior of the magnetic susceptibility suggest a spin-singlet ground state, which is a characteristic property of  $S = 1$  Haldane systems. Due to anisotropy effects, the position of the susceptibility maximum depends on the field orientation. The existence of a finite crystal-field anisotropy in NENB has been confirmed by low-temperature (20 mK) magnetization measurements using the torque-magnetometry technique. Two critical fields ( $B_c^{\parallel} \sim 9$  T and  $B_c^{\perp} \sim 10$  T for  $B$  applied parallel and perpendicular to the  $b$ -axis, respectively) were resolved in the magnetization data (figure 3), suggesting a field-induced collapse of the spin-singlet ground state for both orientations of the magnetic field. The critical fields revealed in our experiments agree well with those obtained from optical and magnetization measurements [17].

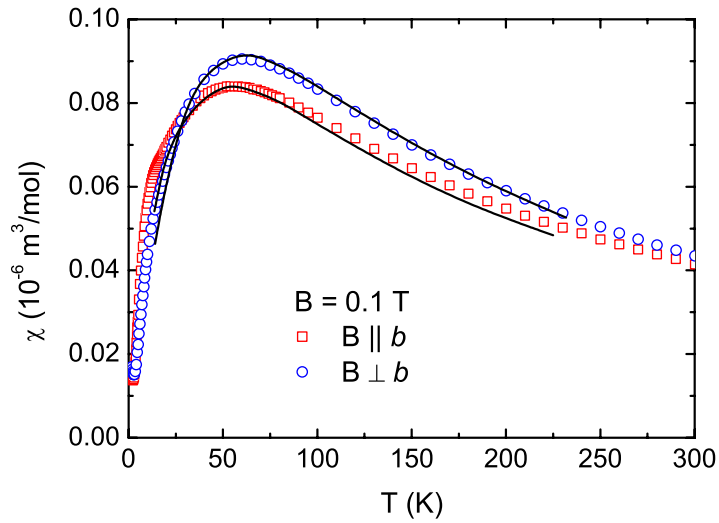


**Figure 2.** Magnetic susceptibility of NENB measured in a magnetic field of 0.1 T, applied along (squares) and perpendicular (circles) to the  $b$ -axis. The solid lines represent calculations using the  $S = 1$  Heisenberg AFM chain model with  $D/J = 0.2$  (see the text for details).

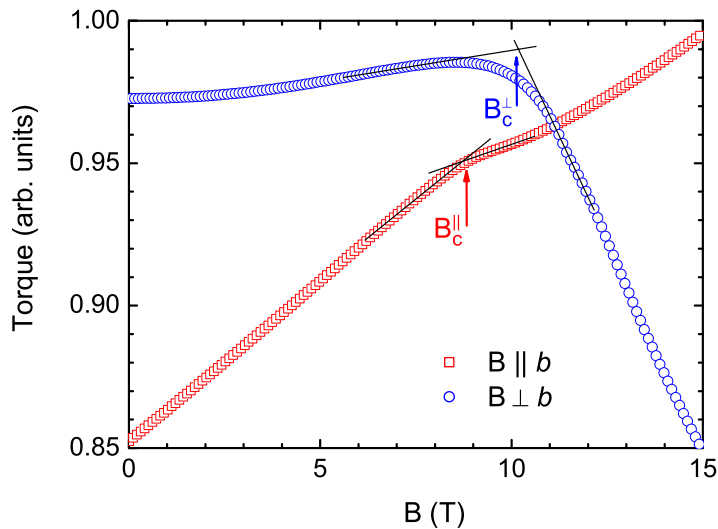


**Figure 3.** Field dependence of the magnetic torque of NENB at 20 mK for two field orientations.

To get a deeper insight into the peculiarity of magnetic interactions in NENB, tunable-frequency ESR measurements have been performed in magnetic fields up to 16 T. The excitation spectrum of NENB in fields parallel to the  $b$ -axis (which is the chain axis) is plotted in figure 4. Several ESR modes have been observed. In order to assign these modes to field-dependent transitions in the energy scheme of magnetic excitations we analyzed the data using the effective spin Hamiltonian, written as [20]

$$\mathcal{H} = \Delta + D'(S_i^z)^2 + E'[(S_i^x)^2 - (S_i^y)^2] - \mu_B S g B \quad (1)$$

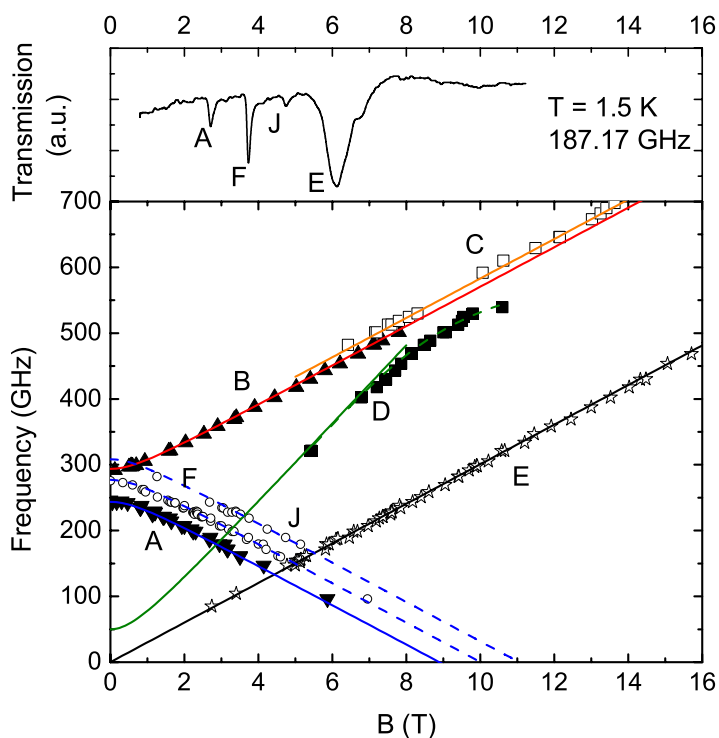


**Figure 4.** Field dependence of the magnetic ESR excitations of NENB observed at 1.5 and 4.3 K with the magnetic field aligned along the  $b$ -axis. Solid lines represent the fit of the effective spin Hamiltonian (equation (1)) to the experimental data. The top part of the figure shows a typical spectrum obtained for 187.17 GHz. The dashed lines are guides to the eyes.

with eigenstates of type  $|S, S^z\rangle$ , where  $\Delta$  is the Haldane gap,  $D'$  and  $E'$  represent reduced parameters of the crystal-field anisotropy (uniaxial- and rhombic-distortion parameters, respectively) of the Ni ions, while the last term is the Zeeman energy.

The field-dependent energy scheme (figure 5) corresponding to this Hamiltonian allows one to understand most of the observed ESR modes. First, the transitions from the ground state to the first excited states ( $|0, 0\rangle \rightarrow |1, \pm 1\rangle$ ), denoted by A and B, have been observed in fields up to  $\sim 8$  T as shown by the triangles in figure 4. The extrapolation of the mode A to zero frequency suggests the existence of a critical field  $B_c^{\parallel} \approx 9$  T, which coincides nicely with the change of the torque signal for fields applied parallel to the  $b$ -axis (figure 3). At this field, the first excited level crosses the nonmagnetic ground state transforming the system into a state with finite magnetization. The transitions A and B would be forbidden in a system with purely axial symmetry, but can be allowed in the presence of staggered magnetization [21]. As suggested by Sakai and Shiba [22], the staggered term lifts wave-vector selection rules and allows transitions from the ground states to the excited states at the boundaries of the Brillouin zone. A staggered magnetic moment may originate from an alternating  $g$  tensor (which was revealed by crystallographic analysis of NENB) or a finite Dzyaloshinskii–Moriya interaction.

The mode D corresponds to transitions  $|1, -1\rangle \rightarrow |1, 1\rangle$ , which are only allowed in the presence of a broken axial symmetry. As follows from our ESR data, the excited doublet is split in zero magnetic field, which is a clear signature of a finite rhombic distortion. The mode C corresponds to  $|1, -1\rangle \rightarrow |1, 0\rangle$  transitions observed in fields above  $\sim 6$  T. The observation

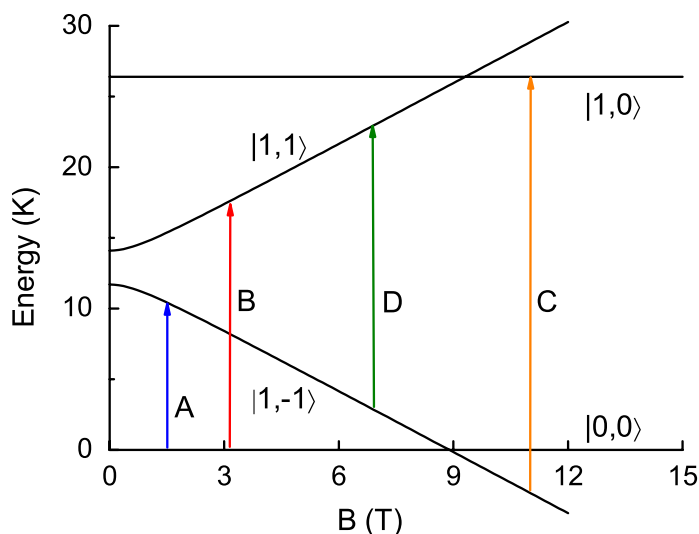


**Figure 5.** Proposed field-dependent energy scheme of NENB (using equation (1)) for magnetic fields applied along the  $b$ -axis.

of this excitation mode is of particular importance, since it gives direct evidence for the four-level excitation scheme, which is a typical feature of an  $S = 1$  Haldane-chain system with finite anisotropy. Then, in accordance with equation (1) for the Haldane gap we found  $\Delta/k_B = 17.4$  K.

Two more resonance absorptions (the modes F and J, figure 4) have been observed in the low-temperature excitation spectrum of NENB. The field dependences of these excitations are similar to that of mode A. The excitation energies are higher by 30 and 60 GHz, for the modes F and J, respectively. The origin of these excitations is not clear at the moment. As mentioned above, the orientation of the nitrite ions within a single chain appears to be uniform (one N atom and one O atom are coordinated to  $\text{Ni}^{2+}$  center along the chain direction). On the other hand, as mentioned in [23], one cannot exclude the possibility of two additional, minor  $\text{Ni}^{2+}$  sites within the chains caused by the reversal of the orientation of the  $\text{NO}_2^-$  groups. This would lead to occasional positions where a  $\text{Ni}^{2+}$  ion in NENB would have either two O atoms from nitrite ions or two N atoms from nitrite ions. Such a possibility was also suggested for the isostructural perchlorate compound NENP [16]. It is important to mention here that additional states close to the Haldane gap were observed in NENP by means of high-field ESR [6, 24], which is fully consistent with our observations. Another possible explanation of the extra states observed by us is the presence of effective ferromagnetic impurity-induced bonds as revealed by susceptibility measurements, see discussion below. Such bonds were found to be responsible for the splitting of the neutron scattering peak into two incommensurate parts placed symmetrically around the boundary of the Brillouin zone close to the gap energy in  $\text{Y}_{2-x}\text{Ca}_x\text{BaNiO}_5$  [25]. However, it is fair to mention that to prove this mechanism to be present in NENB requires more detailed investigations.

Finally, a strong resonance line E, with  $g = 2.14$  was observed. The observation of the mode suggests the presence of spin-1/2 states (their origin can be ascribed to fractional chain-end effects or multiply frustrated interchain interactions) even in nominally pure samples of NENB. These effects, as suggested below, appear to affect the low-temperature magnetic susceptibility.

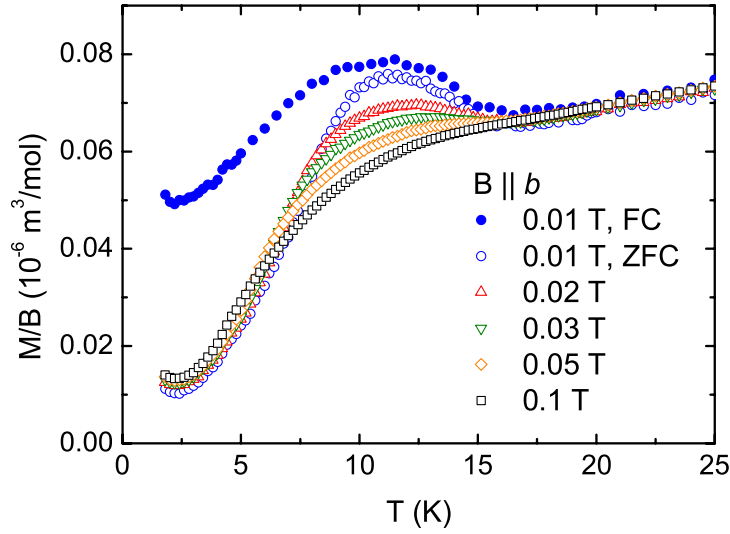


**Figure 6.** Temperature dependence of the magnetic susceptibility of NENB in different magnetic fields applied along the chain  $b$ -axis. Full circles denote susceptibility for the sample cooled in an applied magnetic field of 0.01 T, empty symbols denote ZFC susceptibility.

Using the Hamiltonian equation (1), the ESR data can be fit with the parameters  $\Delta/k_B = 17.4$  K,  $D'/k_B = -13.5$  K,  $|E'/k_B| = 1.2$  K and  $g_{\parallel} = 2.14$ . Numerical calculations for the diagonalization of the Hamiltonian of an  $S = 1$  anisotropic exchange-coupled spin-chain system,

$$\mathcal{H} = -J \sum_i S_i S_{i+1} + \sum_i \{D(S_i^z)^2 + E[(S_i^x)^2 - (S_i^y)^2]\} - \sum_i \mu_B S_i g B, \quad (2)$$

outlined in [6] suggest the relations  $D = -D'/1.8$  and  $|E| = |E'|/1.7$ , which yield the crystal-field anisotropy parameters  $D/k_B = 7.5$  K and  $|E/k_B| = 0.7$  K.

Using the obtained set of parameters, the magnetic susceptibility has been fitted by the high-temperature series expansion for the  $S = 1$  AFM spin-chain model [16, 26] yielding  $J/k_B = -44.8$  K,  $g_{\parallel} = 2.15$  and  $J/k_B = -47.7$  K,  $g_{\perp} = 2.28$  for  $B \parallel b$  and  $B \perp b$ , respectively. The relatively strong crystal-field anisotropy,  $D/k_B = 7.5$  K, as estimated from our ESR data, yields a ratio  $D/|J| = 0.17$ . This suggests that another model (where the influence of anisotropy is taken into account) might be more appropriate for describing the magnetic susceptibility [27]. Although theoretical predictions are available for  $D/|J| = 0.2$ , the overall agreement with the experimentally determined susceptibility data is very good (see figure 2). We obtain  $J/k_B = -45$  K,  $g_{\parallel} = 2.15$  and  $J/k_B = -46.5$  K,  $g_{\perp} = 2.28$  for  $B \parallel b$  and  $B \perp b$ , respectively. Combining these values of the exchange coupling with the ESR results for  $\Delta$  we obtain  $\Delta/|J|$  in the range from 0.39 to 0.42, which is in good agreement with theoretical predictions [3, 4].

The presence of fractional  $S = 1/2$  chain-end spins might be a possible explanation for the observation of the resonance line E in the ESR spectrum as well as for a weak Curie-like low-temperature upturn observed in the susceptibility. The low-temperature susceptibility measured in magnetic fields from 0.01 to 0.1 T (applied parallel to the  $b$ -axis) is shown in figure 6. The susceptibility is characterized by a small but clearly resolvable local maximum at  $\sim 12$  K, which gets rapidly suppressed with increasing magnetic field, and a clear difference between the ZFC

and field-cooled (FC) susceptibility measured with an applied magnetic field of 0.01 T. Such behavior can be accounted for by the formation of a spin-glass state that has also been observed in powdered NENB samples [28].

When structural defects or non-magnetic impurities are introduced in the spin chain, the VBS model predicts the presence of two unpaired  $S = 1/2$  spins, one at each end of the open chain. The existence of these end-chain states has been confirmed numerically (using Monte Carlo [29] and DMRG [30] calculations) as well as experimentally in the Haldane material NENP doped with non-magnetic ions [31]. A pronounced signature of the  $S = 1/2$  chain-end interaction is spin-glass behavior, as observed by Hagiwara *et al* [32, 33], who proposed a model where structural defects induce ferromagnetic bonds between the moments at the ends of finite chains. On the other hand, the structural defects would allow a stronger interchain coupling at the defect sites, which assuming a random distribution of defects appears to induce frustrations and the spin-glass behavior. Additional impurity-induced energy levels were calculated and observed in the quasi-one-dimensional Heisenberg-chain compound  $Y_{2-x}Ca_xBaNiO_5$  [25, 34].

#### 4. Conclusions

In conclusion, a systematic study of the new spin-1 AFM Heisenberg-chain system NENB has been presented. We showed conclusively that NENB belongs to the Haldane class of materials, with the energy gap  $\Delta/k_B = 17.4$  K. Based on the analysis of the ESR and magnetization data, the spin-Hamiltonian parameters have been estimated, yielding the exchange coupling  $J/k_B = -45$  K and crystal-field anisotropy parameters  $D/k_B = 7.5$  K and  $|E/k_B| = 0.7$  K. Extra states in the vicinity of the Haldane gap were observed; their origin is discussed. The presence of fractional  $S = 1/2$  chain-end moments, revealed by means of ESR and magnetization measurements, is found to be responsible for spin-glass freezing effects, which is consistent with the VBS model for  $S = 1$  Heisenberg AFM chains.

#### Acknowledgments

We would like to thank I Affleck for fruitful discussions. Part of this work was supported by the DFG (project no ZV 6/1-1). Part of this work was performed at the National High Magnetic Field Laboratory, Tallahassee, USA, which is supported by NSF Cooperative Agreement no DMR-0084173, by the State of Florida and by the DOE. SAZ acknowledges the support from the NHMFL through the VSP no 1382.

#### References

- [1] Haldane F D M 1983 *Phys. Rev. Lett.* **50** 1153
- [2] Affleck I, Kennedy T, Lieb E H and Tasaki H 1987 *Phys. Rev. Lett.* **59** 799
- [3] White S R and Huse D A 1993 *Phys. Rev. B* **48** 3844
- [4] Gollineli O, Jolicoeur Th and Lacaze R 1994 *Phys. Rev. B* **50** 3037
- [5] Renard J P, Verdaguer M, Regnault L P, Erkelens W A C, Rossat-Mignod J and Stirling W G 1986 *Europhys. Lett.* **3** 945
- [6] Lu W, Tuchendler J, von Ortenberg M and Renard J P 1991 *Phys. Rev. Lett.* **67** 3716
- [7] Darriet J and Regnault L P 1993 *Solid State Commun.* **86** 409
- [8] Yokoo T, Sakaguchi Y, Kakurai K and Akimitsu J 1995 *J. Phys. Soc. Japan* **64** 3651

- [9] Tsujii H, Honda Z, Andraka B, Katsumata K and Takano Y 2005 *Phys. Rev. B* **71** 014426
- [10] Zheludev A, Honda Z, Chen Y, Broholm C L, Katsumata K and Shapiro S M 2002 *Phys. Rev. Lett.* **88** 077206
- [11] Goto T, Ishikawa T, Shimaoka Y and Fujii Y 2006 *Phys. Rev. B* **73** 214406
- [12] Sachdev S, Senthil T and Shankar R 1994 *Phys. Rev. B* **50** 258
- [13] Konik R M and Fendley P 2002 *Phys. Rev. B* **66** 144416
- [14] Affleck I 1991 *Phys. Rev. B* **43** 3215
- [15] Sørensen E S and Affleck I 1993 *Phys. Rev. Lett.* **71** 1633
- [16] Meyer A, Gleizes A, Girerd J-J, Verdaguer M and Kahn O 1982 *Inorg. Chem.* **21** 1729
- [17] Long V C, Chou Y-H, Cross I A, Kozen A C, Montague J R, Schundler E C, Wei X, McGill S A, Landry B R, Maxcy-Pearson K R, Turnbull M M and Landee C P 2007 *Phys. Rev. B* **76** 024439
- [18] Kahn O 1985 *Molecular Magnetism* (New York: Wiley)
- [19] Zvyagin S A, Krzystek J, van Loosdrecht P H M, Dhahlenne G and Revcolevschi A 2004 *Physica B* **346–347** 1
- [20] Date M and Kindo K 1990 *Phys. Rev. Lett.* **65** 1659
- [21] Shiba H, Sakai T, Lüthi B, Palme W and Sieling M 1995 *J. Magn. Magn. Mater.* **140–144** 1590
- [22] Sakai T and Shiba H 1991 *J. Phys. Soc. Japan* **63** 867
- [23] Drew M G B, Goodman D M L, Hitchman M A and Rogers D 1965 *Chem. Commun.* **20** 477
- [24] Sieling M, Palme W and Lüthi B 1995 *Z. Phys. B* **96** 297
- [25] Xu G Y *et al* 2000 *Science* **289** 419
- [26] Weng C Y 1968 *PhD Thesis* Carnegie Institute of Technology
- [27] Yamamoto S and Miyashita S 1994 *Phys. Rev. B* **50** 6277
- [28] Manabe T, Yamashita M, Ohishi T, Yosida T, Yu Y, Honda Z and Katsumata K 1997 *Synth. Met.* **85** 1717
- [29] Miyashita S and Yamamoto S 1993 *Phys. Rev. B* **48** 913
- [30] White S 1992 *Phys. Rev. Lett.* **69** 2863
- [31] Glarum S H, Geschwind S, Lee K M, Kaplan M L and Michel J 1991 *Phys. Rev. Lett.* **67** 1614
- [32] Hagiwara M, Katsumata K, Sasaki S, Narita N, Yamada I and Yosida T 1996 *J. Appl. Phys.* **79** 6167
- [33] Hagiwara M, Narita N and Yamada I 1997 *Phys. Rev. B* **55** 5615
- [34] Lou J Z, Qin S J, Su Z B and Yu L 1998 *Phys. Rev. B* **58** 12672